# First results of the $^{241}$Am(n,f) cross section measurement at the Experimental Area 2 of the n_TOF facility at CERN

*Z.* Eleme[1,*], *N.* Patronis[1], *A.* Stamatopoulos[2], *A.* Tsinganis[3], *M.* Kokkoris[2], *V.* Michalopoulou[2,3], *M.* Diakaki[2,4], *R.* Vlastou[2], *L.* Tassan-Got[2,3,5], *N.* Colonna[6], *J.* Heyse[7], *M.* Barbagallo[3,6], *M.* Mastromarco[3,8], *D.* Macina[3], *E.* Chiaveri[3,8,9], *O.* Aberle[3], *V.* Alcayne[10], *S.* Amaducci[11,12], *J.* Andrzejewski[13], *L.* Audouin[5], *V.* Babiano-Suarez[14], *M.* Bacak[3,15,16], *S.* Bennett[8], *E.* Berthoumieux[16], *D.* Bosnar[17], *A. S.* Brown[18], *M.* Busso[19,20], *M.* Caamaño[21], *L.* Caballero[14], *M.* Calviani[3], *F.* Calviño[22], *D.* Cano-Ott[10], *A.* Casanovas[22], *F.* Cerutti[3], *G. P.* Cortés[22], *M. A.* Cortés-Giraldo[9], *L.* Cosentino[11], *S.* Cristallo[19,23], *L. A.* Damone[6,24], *P. J.* Davies[8], *M.* Dietz[25], *C.* Domingo-Pardo[14], *R.* Dressler[26], *Q.* Ducasse[27], *E.* Dupont[16], *I.* Durán[21], *B.* Fernández-Domíngez[21], *A.* Ferrari[3], *I.* Ferro-Gonçalves[28], *P.* Finocchiaro[11], *V.* Furman[29], *R.* Garg[25], *A.* Gawlik[13], *S.* Gilardoni[3], *K.* Göbel[30], *E.* González-Romero[10], *C.* Guerrero[9], *F.* Gunsing[16], *S.* Heinitz[26], *D. G.* Jenkins[18], *E.* Jericha[15], *U.* Jiri[26], *A.* Junghans[31], *Y.* Kadi[3], *F.* Käppeler[32], *A.* Kimura[33], *I.* Knapová[34], *Y.* Kopatch[29], *M.* Krtička[34], *D.* Kurtulgil[30], *I.* Ladarescu[14], *C.* Lederer-Woods[25], *J.* Lerendegui-Marco[9], *S. J.* Lonsdale[25], *A.* Manna[35,36], *T.* Martínez[10], *A.* Masi[3], *C.* Massimi[35,36], *P. F.* Mastinu[37], *E.* Maugeri[26], *A.* Mazzone[6,38], *E.* Mendoza[10], *A.* Mengoni[35,39], *P. M.* Milazzo[40], *M. A.* Millán-Callado[9], *F.* Mingrone[3], *J.* Moreno-Soto[16], *A.* Musumarra[11,12], *A.* Negret[41], *F.* Ogállar[42], *A.* Oprea[41], *A.* Pavlik[43], *J.* Perkowski[13], *C.* Petrone[41], *L.* Piersanti[19,23], *E.* Pirovano[27], *I.* Porras[42], *J.* Praena[42], *J. M.* Quesada[9], *D.* Ramos Doval[5], *R.* Reifarth[30], *D.* Rochman[26], *C.* Rubbia[3], *M.* Sabaté-Gilarte[9,3], *A.* Saxena[44], *P.* Schillebeeckx[7], *D.* Schumann[26], *A.* Sekhar[8], *A. G.* Smith[8], *N.* Sosnin[8], *P.* Sprung[26], *G.* Tagliente[6], *J. L.* Tain[14], *A. E.* Tarifeño-Saldivia[22], *B.* Thomas[30], *P.* Torres-Sánchez[42], *S.* Urlass[3,31], *S.* Valenta[34], *G.* Vannini[35,36], *V.* Variale[6], *P.* Vaz[28], *A.* Ventura[35], *D.* Vescovi[19,45], *V.* Vlachoudis[3], *A.* Wallner[46], *P. J.* Woods[25], *T. J.* Wright[8], and *P.* Žugec[17]

[1]Department of Physics, University of Ioannina, Greece
[2]Department of Physics, National Technical University of Athens, Greece
[3]European Organization for Nuclear Research (CERN), Switzerland
[4]CEA, DEN, DER/SPRC/LEPh, Cadarache, F-13108 Saint Paul Lez Durance, France
[5]IPN, CNRS-IN2P3, Univ. Paris-Sud, Université Paris-Saclay, F-91406 Orsay Cedex, France
[6]Istituto Nazionale di Fisica Nucleare, Bari, Italy
[7]European Commission, Joint Research Centre, Geel, Retieseweg 111, B-2440 Geel,Belgium
[8]University of Manchester, United Kingdom
[9]Universidad de Sevilla, Spain
[10]Centro de Investigaciones Energéticas Medioambientales y Tecnológicas (CIEMAT), Spain
[11]INFN Laboratori Nazionali del Sud, Catania, Italy
[12]Dipartimento di Fisica e Astronomia, Università di Catania, Italy
[13]University of Lodz, Poland
[14]Instituto de Física Corpuscular, CSIC - Universidad de Valencia, Spain
[15]Technische Universität Wien, Austria
[16]CEA Saclay, Irfu, Université Paris-Saclay, Gif-sur-Yvette, France
[17]Department of Physics, Faculty of Science, University of Zagreb, Croatia
[18]University of York, United Kingdom
[19]Istituto Nazionale di Fisica Nazionale, Perugia, Italy
[20]Dipartimento di Fisica e Geologia, Università di Perugia, Italy
[21]University of Santiago de Compostela, Spain
[22]Universitat Politècnica de Catalunya, Spain
[23]Istituto Nazionale di Astrofisica - Osservatorio Astronomico d'Abruzzo, Italy
[24]Dipartimento di Fisica, Università degli Studi di Bari, Italy
[25]School of Physics and Astronomy, University of Edinburgh, United Kingdom
[26]Paul Scherrer Institut (PSI), Villigen, Switzerland
[27]Physikalisch-Technische Bundesanstalt (PTB), Bundesallee 100, 38116 Braunschweig, Germany
[28]Instituto Superior Técnico, Lisbon, Portugal
[29]Joint Institute for Nuclear Research (JINR), Dubna, Russia
[30]Goethe University Frankfurt, Germany
[31]Helmholtz-Zentrum Dresden-Rossendorf, Germany
[32]Karlsruhe Institute of Technology, Campus North, IKP, 76021 Karlsruhe, Germany
[33]Japan Atomic Energy Agency (JAEA), Tokai-mura, Japan
[34]Charles University, Prague, Czech Republic

[35]Istituto Nazionale di Fisica Nucleare, Sezione di Bologna, Italy
[36]Dipartimento di Fisica e Astronomia, Università di Bologna, Italy
[37]Istituto Nazionale di Fisica Nucleare, Sezione di Legnaro, Italy
[38]Consiglio Nazionale delle Ricerche, Bari, Italy
[39]Agenzia nazionale per le nuove tecnologie, l'energia e lo sviluppo economico sostenibile (ENEA), Bologna, Italy
[40]Istituto Nazionale di Fisica Nazionale, Trieste, Italy
[41]Horia Hulubei National Institute of Physics and Nuclear Engineering (IFIN-HH), Bucharest
[42]University of Granada, Spain
[43]University of Vienna, Faculty of Physics, Vienna, Austria
[44]Bhabha Atomic Research Centre (BARC), India
[45]Gran Sasso Science Institute (GSSI), L'Aquila, Italy
[46]Australian National University, Canberra, Australia

**Abstract.** Feasibility, design and sensitivity studies on innovative nuclear reactors that could address the issue of nuclear waste transmutation using fuels enriched in minor actinides, require high accuracy cross section data for a variety of neutron-induced reactions from thermal energies to several tens of MeV. The isotope $^{241}$Am ($T_{1/2}$= 433 years) is present in high-level nuclear waste (HLW), representing about 1.8 % of the actinide mass in spent PWR UOx fuel. Its importance increases with cooling time due to additional production from the $\beta$-decay of $^{241}$Pu with a half-life of 14.3 years. The production rate of $^{241}$Am in conventional reactors, including its further accumulation through the decay of $^{241}$Pu and its destruction through transmutation/incineration are very important parameters for the design of any recycling solution. In the present work, the $^{241}$Am(n,f) reaction cross-section was measured using Micromegas detectors at the Experimental Area 2 of the n_TOF facility at CERN. For the measurement, the $^{235}$U(n,f) and $^{238}$U(n,f) reference reactions were used for the determination of the neutron flux. In the present work an overview of the experimental setup and the adopted data analysis techniques is given along with preliminary results.

## 1 Introduction

The nuclear power production through ADS (Accelerator Driven Systems) [1] as well as Generation-IV [2] fast neutron reactors is considered as one of the possible solutions that could address the issue of climate change - given the nearly zero $CO_2$ emission rate of nuclear energy compared to other methods of energy production [3]. The same systems provide also the ability of incineration/transmutation of the existing actinides in high-level nuclear waste from spent PWR UOx fuel [4] which is also an important aspect. On the other hand, the safe design and operation of such innovative nuclear power systems is based on accurate nuclear data. One of the most important fissionable isotopes to be considered as a potential candidate for incineration/transmutation is $^{241}$Am ($T_{1/2}$ = 433 y) which represents about 1.8% of the actinide mass in spent fuel. Taking also into account the production rate of $^{241}$Am within spent fuels coming from the $\beta$- decay of $^{241}$Pu ($T_{1/2}$ = 14.3 y) its importance becomes even higher. Accordingly, accurate information of the fission reaction rate of $^{241}$Am for an extended energy region is needed. Therefore, this reaction is included in the Nuclear Energy Agency (NEA) "High Priority Request List" (HPRL) [5] since target accuracies are not yet met by the existing data. The importance of this measurement is also highlighted in the OECD/NEA WPEC Subgroup 26 Final Report [6] that summarizes the needs and target accuracies for nuclear data.

The aforementioned measurement is challenging due to the high specific activity of $^{241}$Am which is 127 MBq/mg and its rapidly increasing cross section above the fission threshold. While a previous measurement at n_TOF in 2003 [7] in the first experimental area (EAR-1) [8], was in good agreement with existing experimental data, due to low statistics the results where given only above the fission threshold and in a rather coarse energy grid.

The enhanced neutron beam intensity of the second experimental area (EAR-2) [9] of the n_TOF facility [10] provides much better signal to background conditions than EAR-1 and high accuracy cross section data can be obtained even at energies below the fission threshold also for high activity samples.

For these reasons, within the present work the study of fission reaction of $^{241}$Am was taken over from the n_TOF Collaboration in EAR-2. In the following sections, the experimental setup is presented along with the adopted data analysis method and preliminary results.

## 2 Experimental Setup

### 2.1 The n_TOF facility

The measurement was carried out at the n_TOF facility at CERN, in the second experimental area (EAR-2) which was commissioned in July 2014. The n_TOF is a Time-Of-Flight facility based on a spallation neutron source. The neutron beams are produced using the pulsed beam of 20GeV/c protons as delivered from the Proton Synchrotron accelerator (PS) of CERN. The beam impinges on a thick cylindrical lead target with dimensions 40 x 60 cm$^2$ (length x diameter). The proton beam has a time width of 7 ns RMS with a maximum repetition rate of 0.8 Hz (1.2 sec between consecutive bunches). The proton accelerator delivers dedicated pulses with a nominal value of ~7 x $10^{12}$ protons/bunch and parasitic ones with reduced intensity by a factor of 2.

The lead target, is surrounded by a 1 cm thick layer of water in constant circulation that serves as coolant and

*e-mail: Zinovia.Eleme@cern.ch

moderator. At 185 m distance horizontally with respect to the lead target, lies the first experimental area (EAR-1), while the second experimental area (EAR-2) is located approximately 20 m above the spallation target and vertical to the direction of the proton beam. Due to its shorter flight path, EAR-2 provides up to 40 times higher neutron flux compared to EAR-1.

The enhanced neutron flux [11] of EAR-2 allows the minimization of the sample thickness while preserving high counting rates. This is crucial when measuring highly radioactive samples, given that the main source of background is attributed to the intrinsic activity of the samples. This is the case in fission studies of several actinides, where the high specific alpha activity becomes the main source of background. The unique combination of high instantaneous flux and high background suppression, provided in EAR-2, allow for accurate fission cross section measurements from thermal energies up to the MeV region.

### 2.2 Samples

The targets used in the measurement were fabricated at JRC- Geel (Belgium). Six samples of $^{241}$Am (99.98% purity) were used with a total mass of 0.78 mg (~4.6 $\mu$g/cm$^2$ per sample) and an activity of ~0.1 GBq. Additionally, for the determination of the neutron flux, two $^{235}$U (0.26 mg, 0.30 mg) with ~9.9 $\mu$g/cm$^2$ per sample and two $^{238}$U (2.07 mg, 2.21 mg) samples with ~75.7 $\mu$g/cm$^2$ per sample, were used as reference foils. In all cases, the sample material was electroplated in a surface 6 cm in diameter on top of an aluminum backing 0.025 mm thick. The sample-backing configuration was mechanically supported by a 2 mm thick aluminum ring 10 cm in diameter.

### 2.3 Detectors

The measurement was carried out using an array of Micromegas detectors (Micro-Mesh Gaseous Structure) which are parallel plate avalanche gaseous detectors that consist of two regions: the conversion (7 mm) and the narrow amplification region (50 $\mu$m) [12]. In the conversion region, which is also referred in literature as drift region, the ionization takes place and charge carriers are directed towards the amplification region where an avalanche multiplication occurs due to the high electric field applied. The two regions are separated by a thin micro-mesh foil, 9.5 cm in diameter with 60 $\mu$m holes on its surface. This is the active area of the detector which is by far larger than the sample diameter (6 cm) as to avoid efficiency losses.

In total ten detectors were used for the measurement: six for the americium and four for the uranium reference samples. The sample-detector modules (Fig.1) were housed in a cylindrical aluminum fission chamber that was filled with a gas mixture of Ar:$CH_4$:isoC$_4$H$_{10}$ (88:10:2) at atmospheric pressure. During the measurement, the gas flow and pressure were monitored and controlled with a dedicated flow-regulator system. In this way, the gas pressure was kept constant ensuring stable gain conditions during the whole data-taking period.

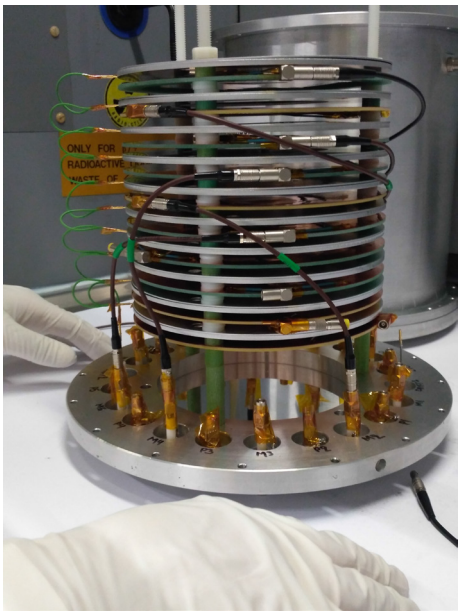

**Figure 1.** The stack of samples and detectors before mounting inside the fission chamber.

### 2.4 Data acquisition

At n_TOF the detector signals are stored as waveforms and digitized. In this way, the characteristics of interest, such as the amplitude, the timing information, the risetime and the full width could be extracted. The raw data for each detector were recorded using a digital acquisition system [13] that was operated using a 112.5 MHz sampling rate in flash Analog-to-Digital Converters (ADC's) with 12 bit resolution (Teledyne SP Devices, model: ADQ412DC [14]). For the data taking, a time acquisition window of 16 ms was adopted. Consequently, experimental data were obtained from a few meV up to the MeV energy region, covering ten orders of magnitude in neutron energy. During data acquisition, a zero suppression algorithm was applied in order to reduce the amount of recorded data.

## 3 Data Analysis

The first step in the data analysis procedure is the processing of raw data of the digitized pulses ("movies"). In this stage, a pulse shape analysis routine was used [15] where the basic characteristics of each pulse are recorded in an event-by-event mode. In this way, the parameters such as the time-of-flight, the amplitude, the rising time, the full-width-at-half-maximum as well as other parameters (33 in total) for each recorded pulse are saved in highly compressed files to be used in the next steps of the data analysis procedure.

The interaction of the proton beam with the spallation lead target results in the generation of $\gamma-$rays and other relativistic particles that reach the experimental areas prior to the arrival of the neutrons. This is commonly referred as "$\gamma-$flash"and causes the creation of a high amplitude signal with a width of a few hundreds of ns. The $\gamma-$flash is accompanied by small oscillations that are diminished

after the first $\mu$s. In energy terms this corresponds to 1-2 MeV. For this reason, a special routine was developed [16] where the average $\gamma$−flash shape for each detector is extracted and then subtracted from the raw data. In this way, pulses generated from fission fragment events could be reconstructed for neutron energies up to a few MeV.

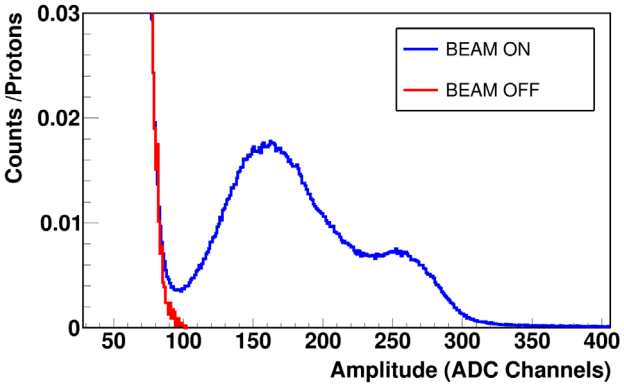


**Figure 2.** An example of beam-on (blue) and beam-off (red) pulse height spectrum for one of the $^{241}$Am targets. As can be seen, the alpha-decay particles are well separated from the fission fragments but still an amplitude threshold has to be applied in the analysis along with the corresponding correction factor.

The second step in the analysis procedure is the accurate determination and implementation of the needed correction factors to the fission yields, in order to accurately estimate the $^{241}$Am fission cross section in an extended energy range. The most important correction factor is the one corresponding to the amplitude cut, applied to the pulse height spectrum so as to isolate the fission events from the alpha particles, attributed to the decay of $^{241}$Am. In this respect, extensive Geant4 [17–19] simulations will be performed to characterize the experimental pulse height spectrum and correct for the applied amplitude cut. To estimate the amplitude threshold, beam-off data were collected as well (Fig.2) during the data-taking period. From these measurements the gain-stability of the detectors was also confirmed.

The excitation function of the $^{241}$Am(n,f) reaction was determined using the $^{235}$U(n,f) and $^{238}$U(n,f) reference reactions for the neutron flux estimation. Preliminary results of the experimental cross section as derived from the weighted average cross section between the six targets of americium can be seen in Fig.3 for the whole energy range covered within the present work.

In Fig.4 preliminary cross section at near threshold energies is presented along with the ENDF/B-VIII.0 [20] and JEFF-3.3 [21] data libraries. Given that the calculation of the needed correction factors is still in progress the data were normalized to the aforementioned data libraries at 1.2 MeV neutron energy. Overall, the trend of the excitation function is in good agreement with the aforementioned data bases and the achieved statistical uncertainty is low enough for fulfilling the accuracy requests for this energy region according to the OECD/NEA WPEC Subgroup 26 Final Report [6].

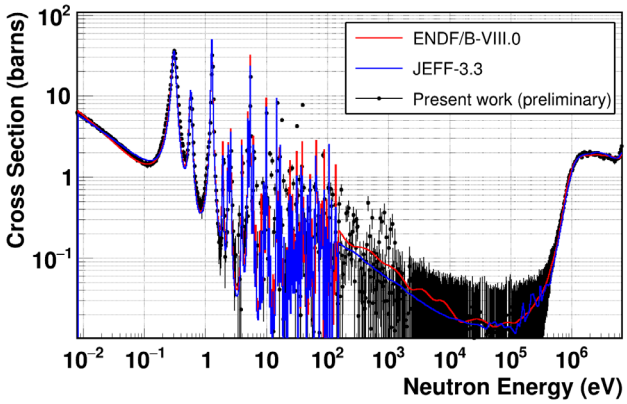


**Figure 3.** Experimental Data of the present work for the $^{241}$Am(n,f) reaction covering the energy range from a few meV up to the MeV region for 60% of the full statistics.

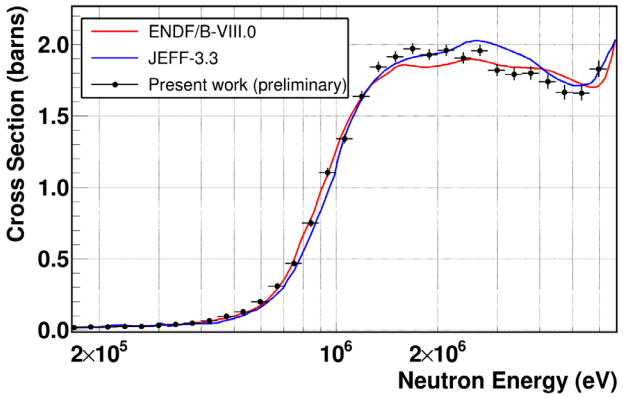


**Figure 4.** Preliminary $^{241}$Am(n,f) cross section derived from the weighted average from the americium samples. The error bars represent the statistical uncertainty. The experimental data are normalized to the evaluated libraries at 1.2 MeV for comparison.

## 4 Conclusions

The $^{241}$Am(n,f) cross section was measured in the second experimental area EAR-2 of the n_TOF facility at CERN with Micromegas detectors. Data are obtained for an extended energy range from thermal up to the MeV region. Preliminary results at near threshold energy region show a good agreement with the evaluated libraries ENDF/B-VIII.0 and JEFF-3.3. The upcoming steps of the data analysis are the accurate determination of the correction factors (amplitude cut, dead-time, possible impurities, etc) so as to calculate the cross section fulfilling the precision requirements for future developments of nuclear energy applications.

## Acknowledgments

This research is co-financed by Greece and the European Union (European Social Fund- ESF) through the Operational Programme «Human Resources Development, Education and Lifelong Learning» in the context of the project “Strengthening Human Resources Research Potential via

Doctorate Research" (MIS-5000432), implemented by the State Scholarships Foundation (IKY).

Also, the authors would like to acknowledge the support of the European Commission under the CHANDA project ($7^{th}$ Framework Programme).

## References

[1] A. Stanculescu, Annals of Nuclear Energy 62, 607-612, (2013)
[2] Generation-IV International Forum, www.gen-4.org/
[3] https://www.iaea.org/sites/default/files/16/11/np-parisagreement.pdf
[4] A.J.M. Plompen, Nucl. Data Sheets 118, 78-84 (2014),
[5] E. Dupont et al., these proceedings, NEA Nuclear Data High Priority Request List, www.nea.fr/html/dbdata/hprl
[6] M. Salvatores et al., OECD/NEA WPEC Subgroup 26 Final Report, www.oecd-nea.org/science/wpec/volume26/volume26.pdf
[7] F. Belloni et al., Eur. Phys. J. A 49, 2 (2013)
[8] C. Guerrero et al., Eur. Phys. J. A 49, 27 (2013)
[9] C. Weiss et al., Nucl. Instrum. Meth. A 799, 90-98 (2015)
[10] C. Rubbia et al., CERN/LHC/98-02 and CERN/LHC/98-02-Add.1 (1998)
[11] M. Sabaté-Gilarte et al., Nucl. Instrum. Meth. A 53, 210 (2017)
[12] S. Andriamonje et al., J. Korean Phys. Soc. 59, 1597 (2011)
[13] U. Abbondanno et al., Nucl. Instrum. Meth. A 538,692-702 (2005)
[14] https://spdevices.com/images/stories/press_releases/15-1404-news_release_spd_cern_20150130.pdf
[15] P. Žugec et al., NIM A 812, 134–144 (2016)
[16] A. Stamatopoulos et al., EPJ Web of Conferences 146, 04030, (2017)
[17] S. Agostinelli et al., Nucl. Instrum. and Methods Phys. Res. A 506, 250-303 (2003)
[18] J. Allison et al., IEEE Transactions on Nuclear Science, vol. 53, issue 1, 270-278 (2006)
[19] J. Allison et al., Nucl. Instrum. and Methods Phys. Res. A 835, 186-225 (2016)
[20] D.A. Brown et al., Nucl. Data Sheets 148, 1 (2018)
[21] Evaluated Data Library 2017, http://www.oecd-nea.org/dbdata/jeff/jeff33/